Thermal noise in optical cavities revisited

Thomas Kessler,[1,2,*] Thomas Legero,[2] and Uwe Sterr[2]

[1]*QUEST Institute for Experimental Quantum Metrology, Physikalisch-Technische Bundesanstalt, Bundesallee 100, 38116 Braunschweig, Germany*
[2]*Physikalisch-Technische Bundesanstalt, Bundesallee 100, 38116 Braunschweig, Germany*
**Corresponding author: thomas.kessler@ptb.de*

Received June 29, 2011; accepted October 18, 2011;
posted October 28, 2011 (Doc. ID 150089); published December 16, 2011

Thermal noise of optical reference cavities sets a fundamental limit to the frequency instability of ultrastable lasers. Using Levin's formulation of the fluctuation-dissipation theorem, we correct the analytical estimate for the spacer contribution given by Numata *et al.* [Phys. Rev. Lett. **93**, 250602 (2004)]. For detailed analysis, finite-element calculations of the thermal noise focusing on the spacer geometry, support structure, and the usage of different materials have been carried out. We find that the increased dissipation close to the contact area between spacer and mirrors can contribute significantly to the thermal noise. From an estimate of the support structure contribution, we give guidelines for a low-noise mounting of the cavity. For mixed-material cavities, we show that the thermal expansion can be compensated without deteriorating the thermal noise.

OCIS codes: 120.2230, 120.3940, 140.3425, 160.2750, 230.5750.

1. INTRODUCTION

Ultrastable optical cavities have become a standard tool for stabilizing laser systems needed, e.g., for high-resolution spectroscopy, optical clocks [1,2], optical microwave generation [3–5], and coherent optical frequency transfer [6–8]. State-of-the-art cavity-stabilized laser systems show linewidths below 1 Hz and fractional frequency instabilities between 10^{-16} and 10^{-15} at 1 s [9–16].

The fractional length stability $\delta L/L$ of ultrastable cavities is limited by inevitable thermal noise in the cavity materials, and a world-wide effort is ongoing to reduce this limitation. An efficient way of calculating thermal noise has been proposed by Levin [17], applying the fluctuation-dissipation theorem. Following his so-called "direct approach" for optical cavities, a set of equations was given by Numata *et al.* [18] for estimating the noise contribution of spacer, substrates, and coatings.

The equations give a good estimate of the thermal noise arising from the mirrors, which have been identified as the dominant source of noise for cavities with mirror substrates made of the widely used ultralow expansion glass (ULE). In state-of-the-art optical cavities, however, substrate materials of higher mechanical quality are being used [16,19–21]. For these optical cavities, a fractional instability on a level of a few 10^{-16} has been shown. At this level, the spacer contribution is nonnegligible and has to be calculated by numerical modeling. In this publication, we describe the mechanisms of dissipation in an optical cavity with focus on the spacer contribution, including the support structure, the usage of different materials, and the spacer geometry. We discuss current cavity designs with respect to their thermal noise budget and, where possible, will give construction guidelines for future cavity designs.

In Section 2 we introduce the theoretical framework used for the simulations. We apply the simulation to a typical cavity design in Subsection 3.A and discuss deviations from the analytical estimate for the spacer contribution. In Subsection 3.B, we show that also the cavity support can lead to nonnegligible contribution to the spacer thermal noise. Finally, in Subsection 3.C, we focus on the thermal noise floor of mixed-material cavities.

2. THEORETICAL FRAMEWORK

Thermal noise in laser mirrors has been investigated in great detail with respect to gravitational wave detection [17,22–28]. A variety of thermal noise sources have been identified so far [29], Brownian thermal noise being the most dominant one. An effective way to estimate thermal noise was first proposed by Levin [17], following the fluctuation-dissipation theorem as introduced by Callen and Welton [30]. The effect of Brownian motion thermal noise on the length stability of ultrastable optical resonators was pointed out by Numata *et al.* [18] following Levin's so-called "direct approach" [17]. This concept is illustrated for clearness in the following.

For optical resonators, the generalized coordinate describing the length fluctuations is the averaged distance between the two cavity mirrors $x = x_1 - x_2$ as probed by the laser field. According to the fluctuation-dissipation theorem, the spectral density $S_x(f)$ of the thermal fluctuations of x is calculated by applying a corresponding conjugate force with amplitude F_0 to each mirror surface, leading to

$$S_x(f) = \frac{2k_B T}{\pi^2 f^2} \frac{W_{\mathrm{diss}}}{F_0^2}, \tag{1}$$

where T denotes the temperature and k_B is the Boltzmann constant. The term W_{diss} denotes the time-averaged dissipated power in the system when an oscillatory force with amplitude F_0 and frequency f is applied. To calculate the thermal noise for a homogeneously distributed internal loss, the term W_{diss} is then expressed by

$$W_{\mathrm{diss}} = 2\pi f U \phi, \tag{2}$$

where U denotes the maximum elastic strain energy and ϕ is the loss angle of the system. The total dissipated power and, thus, the noise of the cavity length x can be described as the sum of the contributions from spacer $S_x^{(\mathrm{sp})}(f)$, two substrates $S_x^{(\mathrm{sb})}(f)$, and two coatings $S_x^{(\mathrm{ct})}(f)$:

$$S_x(f) = \frac{4k_BT}{\pi f F_0^2}(U_{\mathrm{sp}}\phi_{\mathrm{sp}} + 2U_{\mathrm{sb}}\phi_{\mathrm{sb}} + 2U_{\mathrm{ct}}\phi_{\mathrm{ct}}) = S_x^{(\mathrm{sp})}(f) + 2\cdot S_x^{(\mathrm{sb})}(f) + 2\cdot S_x^{(\mathrm{ct})}(f). \quad (3)$$

The power spectral density of length fluctuations $S_x(f)$ can easily be converted to fractional frequency fluctuations $S_y(f) = S_x(f)/L^2$. The instability of the fluctuations in the time domain is conventionally characterized by the Allan deviation σ_y [31] of the fractional frequency fluctuations y. The $1/f$ noise of Eq. (3) (flicker frequency noise) leads to a constant Allan deviation:

$$\sigma_y = \sqrt{2\ln(2)S_y(f)f}. \quad (4)$$

In a typical reference cavity, the differential mirror displacement is probed by a Gaussian laser beam with a $1/e^2$ beam radius w. Consequently, a pressure distribution,

$$p(r) = \pm\frac{2F_0}{\pi w^2}e^{-2r^2/w^2}, \quad (5)$$

has to be applied to the two mirrors with opposite sign to drive the excitation.

If the mirror is treated as an infinite half-space, the contribution of the substrate is given by [17,22]

$$U_{\mathrm{sb}} = \frac{1-\sigma^2}{2\sqrt{\pi}Ew}F_0^2, \qquad S_x^{(\mathrm{sb})}(f) = \frac{4k_BT}{\pi f}\frac{1-\sigma^2}{2\sqrt{\pi}Ew}\phi_{\mathrm{sb}}, \quad (6)$$

where E denotes Young's modulus and σ is the Poisson ratio of the substrate material. Bondu *et al.* [22] later refined the formula for a finite-size mirror, revealing that a long "bar-shaped" mirror substrate with a thickness larger than the mirror radius should be preferred to a "gong-shaped" substrate. However, for typical cavity geometries, the beam waist is much smaller than the mirror dimensions and, therefore, the mirror can be approximated in good accuracy by a infinite half-space.

The coating contribution to Brownian motion thermal noise is typically estimated by treating the coating as a thin layer of thickness d_{ct} on the substrate's front face [26,27,32]. Assuming a homogeneous loss angle ϕ_{ct} and similar elasticity of coating and substrate, as in the case of Ti_2O_5/SiO_2 coatings on ULE or fused silica, the coating contribution reduces to

$$U_{\mathrm{ct}} = U_{\mathrm{sb}}\frac{2}{\sqrt{\pi}}\frac{1-2\sigma}{1-\sigma}\frac{d_{\mathrm{ct}}}{w},$$
$$S_x^{(\mathrm{ct})}(f) = S_x^{(\mathrm{sb})}(f)\frac{2}{\sqrt{\pi}}\frac{1-2\sigma}{1-\sigma}\frac{\phi_{\mathrm{ct}}}{\phi_{\mathrm{sb}}}\frac{d_{\mathrm{ct}}}{w}. \quad (7)$$

For materials with large Young's modulus, such as silicon or sapphire, the thermal noise is dominated by the loss angle for strains perpendicular to the surface, which is difficult to access experimentally (see discussion in [32] for details).

As a rough estimate for the spacer contribution to the cavity noise, the thermal fluctuations of the length of a cylinder, averaged over the whole front face area, are calculated. A cylinder of length L, radius R_{sp}, and central bore radius r_{sp} is assumed. Levin's direct approach then demands a pressure $p = F_0/A_{\mathrm{sp}}$ uniformly distributed across its front faces with area A_{sp}, leading to an elastic energy of

$$U_{\mathrm{sp}}^{(0)} = \frac{L}{2EA_{\mathrm{sp}}}F_0^2 = \frac{L}{2\pi E(R_{\mathrm{sp}}^2 - r_{\mathrm{sp}}^2)}F_0^2. \quad (8)$$

According to Eqs. (1) and (2), the thermal fluctuations of the spacer length L averaged over the full cross section of the front faces are

$$S_L(f) = \frac{4k_BT}{\pi f}\frac{L}{2\pi E(R_{\mathrm{sp}}^2 - r_{\mathrm{sp}}^2)}\phi_{\mathrm{sp}}. \quad (9)$$

Note that this estimate differs from the result given by Numata *et al.* in two ways. First, Eq. (8) takes into account that the front face area of the spacer is reduced by the area of the central bore. Second, our result is a factor of $3/2$ larger than the result by Numata *et al.*. To derive their equation, the authors used the formula for the position fluctuations of one end of a free, elastic bar [33]. This approach is widely employed for single mirrors in interferometers for gravitational wave astronomy. To calculate the length fluctuations of the spacer of a Fabry–Perot interferometer, the authors simply added the fluctuations from both sides, which assumes that those are uncorrelated. According to Levin's direct approach, the calculation of the length fluctuation requires applying opposite forces simultaneously to both ends. Consequently, this approach automatically takes into account correlations from both ends, which were neglected in [18].

According to the model described by Eq. (9), the noise can be minimized by distributing the stress on a large cross section. However, for mirrors smaller than the diameter of the spacer, this approximation is not valid, and for a reliable calculation of the spacer contribution of the thermal noise $S_x^{(\mathrm{sp})}$, finite-element methods (FEMs) have to be applied as described in the next section.

3. SIMULATIONS

For the calculations presented in this section, the software package COMSOL [34] was used. The general cavity geometry is depicted in Fig. 1. The calculations have been carried out in axial symmetry. Because of mirror symmetry with respect to the cavity midplane, half a cavity was simulated. Figure 2 shows the calculated cavity deformation under the pressure distribution of Eq. (5) assuming the parameters given in

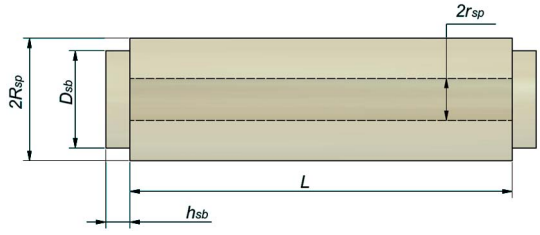

Fig. 1. (Color online) Sketch of the cavity model with dimensions used for the FEM simulations in this publication.

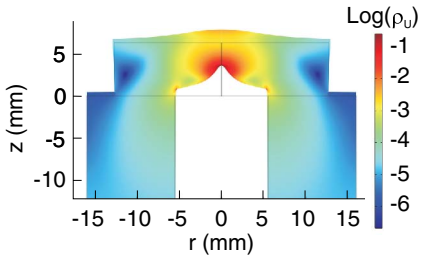

Fig. 2. (Color online) Deformation and contour plot of the elastic strain energy density in the mirror substrate and spacer for a Gaussian pressure profile with a 2 mm waist on the mirror surface. The color coding corresponds to the logarithm of the energy density ρ_U in SI units.

Table 1. For illustration purposes, a beam waist of 2 mm has been chosen. We quote our results in terms of elastic strain energies. For ULE, a strain energy of 1 nJ corresponds to a length fluctuation of $S_L = 8.58 \cdot 10^{-35}\,\mathrm{m^2/Hz}$ at 1 Hz and a corresponding constant Allan deviation of $\sigma_y = 1.09 \cdot 10^{-16}$ for a cavity length of 100 mm. The shape of the deformation of the substrate reflects the Gaussian beam profile. The majority of the elastic strain energy is stored in the cavity substrate. Strong local deformations occur at the boundary between substrate and spacer, extending into the spacer. At a distance exceeding this critical depth, a homogeneous energy density distribution is obtained.

A. Local Spacer Deformations

Following the discussion of Fig. 2, it is clear that the analytic estimate for the spacer contribution according to Eq. (8) cannot hold for the full spacer length as it neglects local deformations arising from the nonuniform pressure distribution on its front face.

To illustrate the size of the effect, we estimate and simulate the thermal noise following Eqs. (6)–(8) for an all-ULE cavity with the dimensions and material parameters given in Table 1. The results of the calculation are shown in Table 2. The major part of the total strain energy caused by the static deformation is stored in the substrates. The contribution of the substrate is in good agreement with the analytic Eqs. (6) on the level of 1%. This result reflects the good approximation of the mirror surface treated as an infinite half-space, i.e., the beam waist being much smaller than the mirror dimensions. The coating contribution was estimated by Eq. (7) for both the analytic calculation and the simulation. For the spacer geometry given

Table 1. Parameters Used for the FEM Simulation

R_{sp}	spacer radius	16 mm
L	spacer length	100 mm
r_{sp}	spacer central bore radius	5.5 mm
D_{sb}	substrate diameter	25.4 mm
h_{sb}	substrate thickness	6.3 mm
d_{ct}	coating thickness	2 μm
w	beam waist ($1/e^2$ radius)	240 μm
E	Young's modulus ULE (FS)	67.6 (73.0) GPa
ν	Poisson's ratio ULE (FS)	0.17 (0.16)
ϕ_{ct}	loss angle coating	$4 \cdot 10^{-4}$
$1/\phi$	quality factor ULE (FS)	$6 \cdot 10^4$ (10^6)
T	temperature	293 K
k_B	Boltzmann's constant	$1.381 \cdot 10^{-23}$ J/K

Table 2. Comparison of Strain Energies in Nanojoules for an All-ULE Cavity

	Spacer	Substrate	Coating
Analytic result	1.04	16.89	0.126
FEM calculation	1.50	16.99	0.127

in Table 1, Eq. (8) underestimates the energy stored in the spacer by approximately 30%. To shine light on this mismatch, it is illustrative to calculate the energy distribution along the spacer length. The resulting graph for slices with a thickness of 1 mm is shown in Fig. 3. The results have been normalized to the energy U_0 contained in a slice of a homogeneously loaded spacer, as described by Eq. (8) in Section 2. While the energy stored in the central part of the spacer matches the value predicted by Eq. (8), excess energy from additional deformations is stored close to the mirror. The penetration depth amounts to roughly 10 mm. The excess energy can be attributed to stress acting nonuniformly on the front face of the spacer, as illustrated in Fig. 2. The analytic estimate can be reproduced by applying a homogeneous force along the spacer's front face as expected. The amount of excess energy on the spacer ends depends on the design parameters of the cavity.

The dependence of the strain energy on the length of the cavity is shown in Fig. 4 in comparison with the analytic estimates from Eq. (8) and from [18]. For cavities longer than the penetration depth of the local deformation of roughly 10 mm, the simulation data are offset from the analytic estimate by a constant excess energy of approximately 0.45 nJ. Thus, once the elastic strain energy caused by the local deformations at the spacer's front faces has been determined for a given cavity geometry, the elastic energy of a cavity of a different length can be calculated according to Eq. (8). As the analytic estimate predicts the energy to be proportional to L, the effect of the local deformations becomes negligible for long spacers.

The dependence of the strain energy on the spacer diameter is illustrated in Fig. 5 in comparison to the $1/R_{sp}^2$ dependence of the analytic result {(Eq. (8) and [18]}. All three curves show a decrease of the strain energy with increasing spacer diameter. The excess energy increases from 0.45 nJ for a diameter of 32 mm, as given in the example before, and saturates at ~0.8 nJ for a spacer diameter approaching 100 mm.

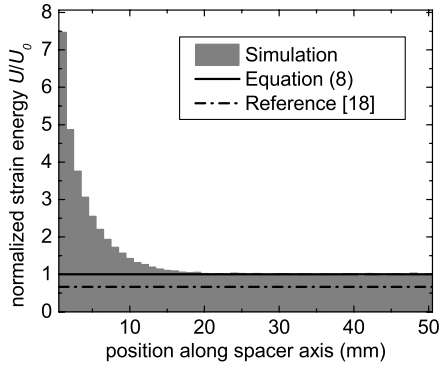

Fig. 3. Simulated strain energy in slices of 1 mm thickness compared to a homogeneously loaded spacer (U_0) [see Eq. (8)]. The estimate by Numata *et al.* [18] (dashed–dotted line) and the analytic estimate according to Eq. (8) (solid line) are shown as references.

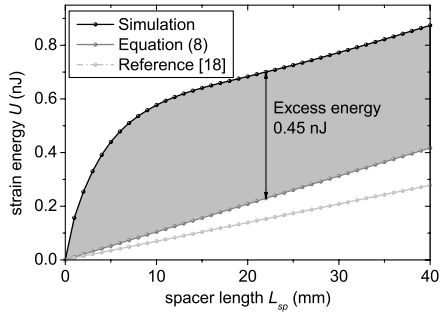

Fig. 4. Strain energy as a function of spacer length for a spacer diameter of 32 mm. The estimate by Numata *et al.* [18] (dashed–dotted curve) as well as the analytic estimate according to Eq. (8) (solid curve) are shown as a reference.

Note that, for those diameters, the spacer energy is totally dominated by the excess energy close to the mirrors ends.

In summary, Eq. (8) holds for the central region of the spacer while it fails close to the spacer ends. The impact of the spacer contribution on the total thermal noise budget of the cavity is small for all-ULE cavities, where the dominant part of the noise arises from the mirrors. However, it can be strongly enhanced if the spacer's mechanical losses exceed the ones for the mirrors (see Subsection 3.C) or if nearly confocal cavities with large beam waists on the mirror surface lead to a reduction of the mirror thermal noise. In these cases, a careful treatment of the spacer noise in a finite-element analysis is mandatory.

B. Support Structure

To obtain fractional frequency instabilities below $\sigma_y = 10^{-15}$, modern optical cavities employ vibration insensitive mountings [4,13,35,36]. In one widely used design for horizontal cavities, the resonators are supported at four positions close to the Airy points by elastic materials [9,13,36,37]. As the mechanical quality factor of rubber-type material is relatively low, the contribution of the support to the thermal noise might not be negligible. To estimate the thermal noise contribution from an elastic support, we investigate the geometry depicted in Fig. 6.

A spacer of length L is supported by four rubber supports of thickness d_{sup}, area A_{sup}, and shear modulus G_{sup} at the Airy points positioned symmetrically at a distance L_{sup} from the center. As the pads are located far from the spacer's front faces, local spacer deformations, as discussed in Subsection 3.A,

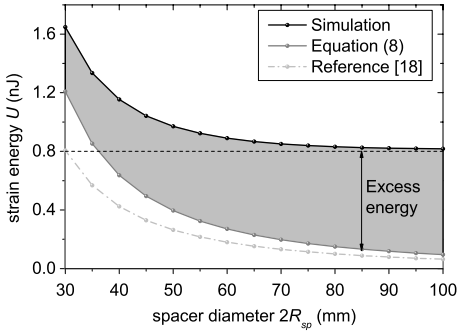

Fig. 5. Elastic strain energy as a function of spacer diameter for a spacer length of 100 mm. The estimate by Numata *et al.* [18] (dashed–dotted curve) as well as the analytic estimate according to Eq. (8) (solid curve) are shown as references.

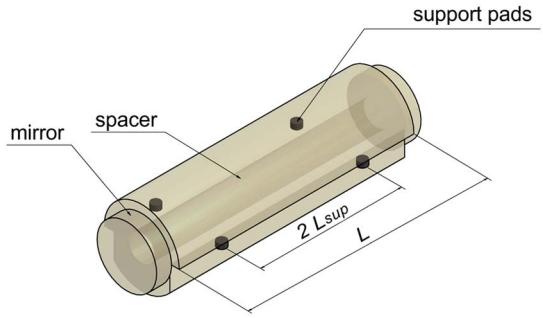

Fig. 6. (Color online) Sketch of a cavity supported by four elastic support pads.

can be neglected, and we can treat the spacer as a homogeneously loaded bar. We again use the fluctuation-dissipation theorem in the form of Eq. (1) to estimate the thermal noise contribution from the supports. We can estimate the energy stored in the support structure by assuming that the contact surfaces of the support and spacer are displaced along the spacer axis direction according to the elastic expansion of the spacer. The support pads are placed at a distance L_{sup} from the center of the spacer. Opposite forces F_0 applied on the front faces of the spacer displace each rubber surface by

$$\delta L_{\mathrm{sup}} = \frac{L_{\mathrm{sup}}}{A_{\mathrm{sp}} E_{\mathrm{sp}}} F_0. \tag{10}$$

If we assume the support pads to be fixed to the support structure and have negligible action back on the deformation of the spacer, the resulting shear energy for a support pad is given by

$$U_{\mathrm{sup}} = \frac{1}{2}\frac{A_{\mathrm{sup}} G_{\mathrm{sup}}}{d_{\mathrm{sup}}} \delta L_{\mathrm{sup}}^2 \approx \frac{A_{\mathrm{sup}}}{A_{\mathrm{sp}}} \frac{L_{\mathrm{sup}}}{d_{\mathrm{sup}}} \frac{G_{\mathrm{sup}}}{E_{\mathrm{sp}}} \frac{L_{\mathrm{sup}}}{L} U_{\mathrm{sp}}^{(0)}. \tag{11}$$

In this approximation, the shear energy is only affected by the shear strain and the displacement of the boundary is given by the spacer displacement itself. As a result, a support with small area A_{sup}, large thickness d_{sup}, and small shear modulus G_{sup} will reduce the strain energy and, therefore, the thermal noise. The thermal noise contribution from four support points is then estimated by

$$S_x^{(\mathrm{sup})}(f) = 4\frac{4k_B T}{\pi f F_0^2} U_{\mathrm{sup}} \phi_{\mathrm{sup}} = 4\frac{A_{\mathrm{sup}}}{A_{\mathrm{sp}}} \frac{L_{\mathrm{sup}}}{d_{\mathrm{sup}}} \frac{G_{\mathrm{sup}}}{E_{\mathrm{sp}}} \frac{L_{\mathrm{sup}}}{L} \frac{\phi_{\mathrm{sup}}}{\phi_{\mathrm{sp}}} S_L(f). \tag{12}$$

The distance of the support from the center can be estimated for an elastic bar by $L_{\mathrm{sup}} = L/(2\sqrt{3})$ according to [38]. Consequently, the displacement noise $S_{\mathrm{sup}}(f)$ for the support is proportional to L^2, resulting in a fractional displacement noise $S_y^{(\mathrm{sup})}(f) = S_x^{(\mathrm{sup})}(f)/L^2$ independent of the cavity length. Therefore, care has to be taken, especially for long spacers, to avoid excessive influence of the support on the total noise budget.

For a vertical mounting of the cavity at the midplane (see, e.g., [12,20]) the shear of the support pads acts transversal to the driving force deforming the spacer and the strain energy [Eq. (11)] is reduced by a factor of $(\sigma_{\mathrm{sp}} \cdot 2R_c/L)^2$.

Table 3. Parameters for Simulation of the Cavity Support

A_{sup}	area	$2\,mm^2$	[16]
d_{sup}	thickness	0.7 mm	[16]
E_{sup}	Young's modulus	0.8 MPa	
ν_{sup}	Poisson's ratio	0.27	
G_{sup}	shear modulus	$E_{sup}/(2+2\nu_{sup}) = 0.31\,MPa$	[44]
ϕ_{sup}	loss angle	0.33	[44,45]

For the horizontal cavity design with the parameters given in Tables 3 and 1, we can estimate that the support of four Viton pads amounts to roughly 1% of the displacement noise $S_L(f) = 8.95 \cdot 10^{-35}/f\,m^2/Hz$ created in an ULE spacer. For spacer materials of higher mechanical quality, however, the ratio ϕ_{sup}/ϕ_{sp} can increase drastically and, therefore, in future cavity designs the importance of the mounting scheme will increase. For a cavity made of silicon, for example, Young's modulus in the [111] direction is 188 GPa [39] and the mechanical loss angle of the material is $\phi = 2 \cdot 10^{-8}$ [40], about 3 orders of magnitude below the one for ULE (see Table 1). Consequently, for a cavity made out of silicon, the total thermal noise of the four support pads exceeds the noise of the spacer by a factor of ~4. Cavities of this type of material are currently limited entirely by the coating noise. However, once low-loss coatings with sufficient reflectivities [41] are available, this picture might change.

C. Mixed-Material Cavities

In current cavities with ULE mirrors, the major contribution to the cavity's thermal noise arises from their mirror substrates. Substrate materials of higher mechanical Q-factor, like fused silica (FS), have been used [16,19] to reduce this noise contribution. The thermal noise of FS mirrors is already dominated by the noise of the coating (compare Fig. 7). However, FS shows a relatively large room-temperature coefficient of thermal expansion (CTE) of around $5 \cdot 10^{-7}/K$. The large CTE difference in such a mixed-material cavity leads to an unwanted lowering of the zero crossing temperature of the cavity's CTE of the order of a few 10 K. To compensate for this effect, either special mirror configurations have been applied [35] or additional ULE rings have been optically contacted to the back surfaces of the FS mirrors [19].

We use the FEM model discussed in Subsection 3.A to check whether the additional ULE rings of the latter approach corrupt the low thermal noise of the FS mirrors. To the cavity model shown in Fig. 1, additional 6 mm thick ULE rings with a diameter of 25.4 mm and a central bore of 9 mm have been added. Figure 7 shows the FEM results of the thermal noise contributions of the different cavity components. We find that the additional thermal noise of the ULE ring is much smaller than the noise contribution of the mirror substrate or the mirror coating. The ULE rings enlarge the effective thickness of the mirrors, which results in a smaller spacer deformation and, therefore, in a smaller spacer excess energy. This reduction in the corresponding thermal noise is even bigger than the additional thermal noise contribution of the rings itself and we have the paradoxical situation that a combined material cavity with additional ULE rings shows less thermal noise than without these rings.

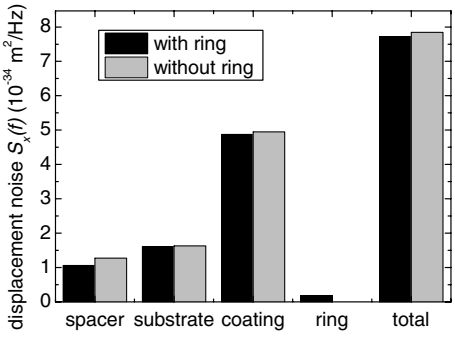

Fig. 7. Contributions to the thermal noise of the optical length $S_x(f)$ of a cavity with and without a thermal expansion compensation ring.

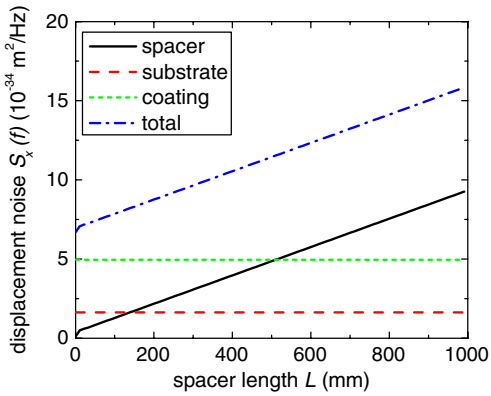

Fig. 8. (Color online) Contributions to the thermal noise of the optical length $S_x(f)$ as function of the spacer length L.

While for all-ULE cavities, the spacer contribution is negligible, in mixed-material cavities, the ULE spacer starts limiting the performance of the cavity. In general, following the discussion from Section 2, the noise contribution from the spacer is proportional to L and, consequently, a length L can be found where the spacer contribution equals the mirror contribution. This effect is illustrated for an FS-type substrate in Fig. 8. For a cavity with the parameters given in Table 1, this length would correspond to 500 mm.

4. CONCLUSION

Following Levin's "direct approach," we have analyzed the fractional length change of state-of-the-art optical cavities driven by Brownian motion thermal noise. While the thermal noise contribution created by the mirror is in good agreement with analytic results, we find discrepancies to the estimates given in [18] for the spacer contribution. We give a revised analytic equation valid for long spacers and find an additional contribution because of additional deformations at the spacer ends close to the mirrors. This excess energy can exceed the energy deposited by linear elastic deformation and can dominate the spacer contribution to the thermal noise for large spacer diameters and also for short spacer lengths.

Another nonnegligible source for thermal noise can arise from the support structure of the material. We have given estimate equations for a cavity mounted on soft support pads from below.

Finally, we have investigated the thermal noise of mixed-material cavities. We confirm that an additional compensator ring made of ULE (see [19]) has no effect on the total cavity thermal noise.

Current cavities are mostly limited by the coating noise. However, this may change as low-loss coatings are being developed, like microstructured mirrors [41] or coatings based on monocrystalline $Al_xGa_{1-x}As$ heterostructures [42]. Additional reduction of thermal noise may by achieved by using large mode diameters or higher-order transversal modes [43]. In these cases, the results given in this publication enable further reduction of the thermal noise from the spacer, e.g., using thick mirrors, long cavities, and optimized mounting. With these precautions, instabilities below 10^{-16} seem to be possible.

ACKNOWLEDGMENTS

We acknowledge financial support by the Centre for Quantum Engineering and Space-Time Research (QUEST). This work is supported by the European Community's ERA-NET-Plus Programme under Grant Agreement No. 217257, by the European Space Agency (ESA), and Deutsches Zentrum für Luft- und Raumfahrt (DLR) in the project *Space Optical Clocks*.

REFERENCES

1. T. Rosenband, D. B. Hume, P. O. Schmidt, C. W. Chou, A. Brusch, L. Lorini, W. H. Oskay, R. E. Drullinger, T. M. Fortier, J. E. Stalnaker, S. A. Diddams, W. C. Swann, N. R. Newbury, W. M. Itano, D. J. Wineland, and J. C. Bergquist, "Frequency ratio of Al^+ and Hg^+ single-ion optical clocks; metrology at the 17th decimal place," Science **319**, 1808–1812 (2008).
2. A. D. Ludlow, T. Zelevinsky, G. K. Campbell, S. Blatt, M. M. Boyd, M. H. G. de Miranda, M. J. Martin, J. W. Thomsen, S. M. Foreman, J. Ye, T. M. Fortier, J. E. Stalnaker, S. A. Diddams, Y. Le Coq, Z. W. Barber, N. Poli, N. D. Lemke, K. M. Beck, and C. W. Oates, "Sr lattice clock at 1×10^{-16} fractional uncertainty by remote optical evaluation with a Ca clock," Science **319**, 1805–1808 (2008).
3. A. Bartels, S. A. Diddams, C. W. Oates, G. Wilpers, J. C. Bergquist, W. H. Oskay, and L. Hollberg, "Femtosecond-laser-based synthesis of ultrastable microwave signals from optical frequency references," Opt. Lett. **30**, 667–669 (2005).
4. J. Millo, M. Abgrall, M. Lours, E. English, H. Jiang, J. Guéna, A. Clairon, S. Bize, Y. L. Coq, G. Santarelli, and M. Tobar, "Ultra-low noise microwave generation with fiber-based optical frequency comb and application to atomic fountain clock," Opt. Lett. **34**, 3707–3709 (2009).
5. B. Lipphardt, G. Grosche, U. Sterr, C. Tamm, S. Weyers, and H. Schnatz, "The stability of an optical clock laser transferred to the interrogation oscillator for a Cs fountain," IEEE Trans. Instrum. Meas. **58**, 1258–1262 (2009).
6. P. A. Williams, W. C. Swann, and N. R. Newbury, "High-stability transfer of an optical frequency over long fiber-optic links," J. Opt. Soc. Am. B **25**, 1284–1293 (2008).
7. H. Jiang, F. Kéfélian, S. Crane, O. Lopez, M. Lours, J. Millo, D. Holleville, P. Lemonde, C. Chardonnet, A. Amy-Klein, and G. Santarelli, "Transfer of an optical frequency over an urban fiber link," J. Opt. Soc. Am. B **25**, 2029–2035 (2008).
8. O. Terra, G. Grosche, K. Predehl, R. Holzwarth, T. Legero, U. Sterr, B. Lipphardt, and H. Schnatz, "Phase-coherent comparison of two optical frequency standards over 146 km using a telecommunication fiber link," Appl. Phys. B **97**, 541–551 (2009).
9. B. C. Young, F. C. Cruz, W. M. Itano, and J. C. Bergquist, "Visible lasers with subhertz linewidths," Phys. Rev. Lett. **82**, 3799–3802 (1999).
10. H. Stoehr, F. Mensing, J. Helmcke, and U. Sterr, "Diode laser with 1 Hz linewidth," Opt. Lett. **31**, 736–738 (2006).
11. M. Notcutt, L.-S. Ma, A. D. Ludlow, S. M. Foreman, J. Ye, and J. L. Hall, "Contribution of thermal noise to frequency stability of rigid optical cavity via Hertz-linewidth lasers," Phys. Rev. A **73**, 031804 (2006).
12. A. D. Ludlow, X. Huang, M. Notcutt, T. Zanon-Willette, S. M. Foreman, M. M. Boyd, S. Blatt, and J. Ye, "Compact, thermal-noise-limited optical cavity for diode laser stabilization at 1×10^{-15}," Opt. Lett. **32**, 641–643 (2007).
13. S. A. Webster, M. Oxborrow, S. Pugla, J. Millo, and P. Gill, "Thermal-noise-limited optical cavity," Phys. Rev. A **77**, 033847 (2008).
14. P. Dubé, A. Madej, J. Bernard, L. Marmet, and A. Shiner, "A narrow linewidth and frequency-stable probe laser source for the $^{88}Sr^+$ single ion optical frequency standard," Appl. Phys. B **95**, 43–54 (2009).
15. J. Lodewyck, P. G. Westergaard, A. Lecallier, L. Lorini, and P. Lemonde, "Frequency stability of optical lattice clocks," New J. Phys. **12**, 065026 (2010).
16. J. Millo, D. V. Magalhães, C. Mandache, Y. Le Coq, E. M. L. English, P. G. Westergaard, J. Lodewyck, S. Bize, P. Lemonde, and G. Santarelli, "Ultrastable lasers based on vibration insensitive cavities," Phys. Rev. A **79**, 053829 (2009).
17. Y. Levin, "Internal thermal noise in the LIGO test masses: a direct approach," Phys. Rev. D **57**, 659–663 (1998).
18. K. Numata, A. Kemery, and J. Camp, "Thermal-noise limit in the frequency stabilization of lasers with rigid cavities," Phys. Rev. Lett. **93**, 250602 (2004).
19. T. Legero, T. Kessler, and U. Sterr, "Tuning the thermal expansion properties of optical reference cavities with fused silica mirrors," J. Opt. Soc. Am. B **27**, 914–919 (2010).
20. T. Kessler, "Development of an ultrastable monocrystalline silicon resonator for optical clocks," presented at the European Frequency and Time Forum 2010, Noordwijk, The Netherlands, 13–16 April 2010.
21. M. Notcutt, C. T. Taylor, A. G. Mann, and D. G. Blair, "Temperature compensation for cryogenic cavity stabilized lasers," J. Phys. D **28**, 1807–1810 (1995).
22. F. Bondu, P. Hello, and J.-Y. Vinet, "Thermal noise in mirrors of interferometric gravitational wave antennas," Phys. Lett. A **246**, 227–236 (1998).
23. V. B. Braginsky, M. L. Gorodetsky, and S. P. Vyatchanin, "Thermodynamical fluctuations and photo-thermal shot noise in gravitational wave antennae," Phys. Lett. A **264**, 1–10 (1999).
24. Y. T. Liu and K. S. Thorne, "Thermoelastic noise and homogeneous thermal noise in finite sized gravitational-wave test masses," Phys. Rev. D **62**, 122002 (2000).
25. V. B. Braginsky and S. P. Vyatchanin, "Thermodynamical fluctuations in optical mirror coatings," Phys. Lett. A **312**, 244–255 (2003).
26. M. M. Fejer, S. Rowan, G. Cagnoli, D. R. M. Crooks, A. Gretarsson, G. M. Harry, J. Hough, S. D. Penn, P. H. Sneddon, and S. P. Vyatchanin, "Thermoelastic dissipation in inhomogeneous media: loss measurements and displacement noise in coated test masses for interferometric gravitational wave detectors," Phys. Rev. D **70**, 082003 (2004).
27. M. Evans, S. Ballmer, M. Fejer, P. Fritschel, G. Harry, and G. Ogin, "Thermo-optic noise in coated mirrors for high-precision optical measurements," Phys. Rev. D **78**, 102003 (2008).
28. Y. Levin, "Fluctuation-dissipation theorem for thermo-refractive noise," Phys. Lett. A **372**, 1941–1944 (2008).
29. M. L. Gorodetsky, "Thermal noises and noise compensation in high-reflection multilayer coating," Phys. Lett. A **372**, 6813–6822 (2008).
30. H. B. Callen and T. A. Welton, "Irreversibility and generalized noise," Phys. Rev. **83**, 34–40 (1951).
31. D. W. Allan, "Statistics of atomic frequency standards," Proc. IEEE **54**, 221–230 (1966).
32. G. M. Harry, A. M. Gretarsson, P. R. Saulson, S. E. Kittelberger, S. D. Penn, W. J. Startin, S. Rowan, M. M. Fejer, D. R. M. Crooks, G. Cagnoli, J. Hough, and N. Nakagawa, "Thermal noise in interferometric gravitational wave detectors due to dielectric optical coatings," Class. Quantum Grav. **19**, 897–917 (2002).
33. K. Yamamoto, "Study of the thermal noise caused by inhomogeneously distributed loss," Ph.D. dissertation (University of Tokyo, 2000).
34. COMSOL AB, "COMSOL Multiphysics Version 4.1" (2010).
35. S. A. Webster and P. Gill, "Low-thermal-noise optical cavity," in *Proceedings of the 2010 IEEE International Frequency Control Symposium* (2010), pp. 470–473.

36. T. Nazarova, F. Riehle, and U. Sterr, "Vibration-insensitive reference cavity for an ultra-narrow-linewidth laser," Appl. Phys. B **83**, 531–536 (2006).
37. S. A. Webster, M. Oxborrow, and P. Gill, "Vibration insensitive optical cavity," Phys. Rev. A **75**, 011801(R) (2007).
38. F. Phelps, "Airy points of a meter bar," Am. J. Phys. **34**, 419–422 (1966).
39. J. J. Wortman and R. A. Evans, "Young's modulus, shear modulus, and Poisson's ratio in silicon and germanium," J. Appl. Phys. **36**, 153–156 (1965).
40. D. F. McGuigan, C. C. Lam, R. Q. Gram, A. W. Hoffman, D. H. Douglass, and H. W. Gutche, "Measurements of the mechanical *Q* of single-crystal silicon at low temperatures," J. Low Temp. Phys. **30**, 621–629 (1978).
41. F. Brückner, D. Friedrich, T. Clausnitzer, M. Britzger, O. Burmeister, K. Danzmann, E.-B. Kley, A. Tünnermann, and R. Schnabel, "Realization of a monolithic high-reflectivity cavity mirror from a single silicon crystal," Phys. Rev. Lett. **104**, 163903 (2010).
42. G. D. Cole, S. Gröblacher, K. Gugler, S. Gigan, and M. Aspelmeyer, "Monocrystalline $Al_xGa_{1-x}As$ heterostructures for high-reflectivity high-*Q* micromechanical resonators in the megahertz regime," Appl. Phys. Lett. **92**, 261108 (2008).
43. B. Mours, E. Tournefier, and J.-Y. Vinet, "Thermal noise reduction in interferometric gravitational wave antennas: using high order TEM modes," Class. Quantum Grav. **23**, 5777–5784 (2006).
44. D. Hoffman, "Dynamic mechanical signatures of Viton A and plastic bonded explosives based on this polymer," Polym. Eng. Sci. **43**, 139–156 (2003).
45. J. Giaime, P. Saha, D. Shoemaker, and L. Sievers, "A passive vibration isolation stack for LIGO: design, modeling, and testing," Rev. Sci. Instrum. **67**, 208–214 (1996).